OVERVIEW OF ADVANCED WING DESIGN

Raymond M. Hicks

NASA Ames Research Center

ABSTRACT

Several recent examples of experiment-theory correlation are presented to give an indication of the capabilities and limitations of wing design and analysis for transonic applications by potential-flow theory. The examples include correlations of experimental pressure distributions with theoretical results from isolated wing codes and wing-body codes. Both conservative and non-conservative differencing as well as body and boundary layer corrections are considered. The results show that a full potential isolated wing code correlates well with data from an isolated wing test but may give poor prediction of the aerodynamic characteristics of some wing-body configurations. Potential-flow wing body codes were found to improve the correlation for the wing-body configurations considered.

ISOLATED WING WIND TUNNEL MODEL

The swept wing shown in Figure 1 was tested in the Ames 12-foot pressure tunnel at Mach .8 and at Reynolds number of 2 million based on the M.A.C. (ref. 1). The model was mounted on the tunnel wall and hence is useful for evaluating isolated wing codes.

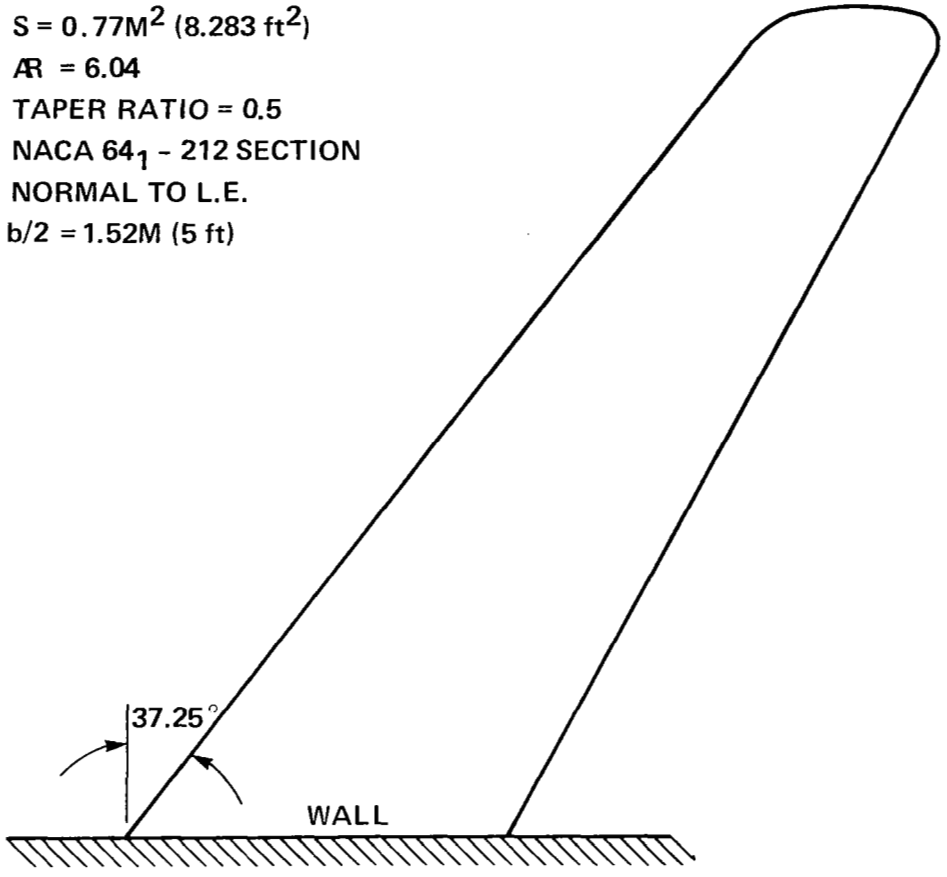

Figure 1

EXPERIMENT-THEORY CORRELATION FOR AN ISOLATED WING

The experiment-theory correlation for the isolated wing is shown in Fig. 2. The code FLO22NM solves the transonic potential equation in non-conservative form with an iterated Nash-McDonald boundary layer correction. The boundary layer subroutine was coupled with FLO22 by P. A. Henne of Douglas Aircraft Company. The results shown in the figure indicate that good experiment-theory correlation of wing pressures can be expected for most isolated wings with 6-series sections at span stations greater than $\eta \sim .15$. The correlation might be expected to be less satisfactory at span stations closer to the wall due to the close proximity to the tunnel wall boundary layer.

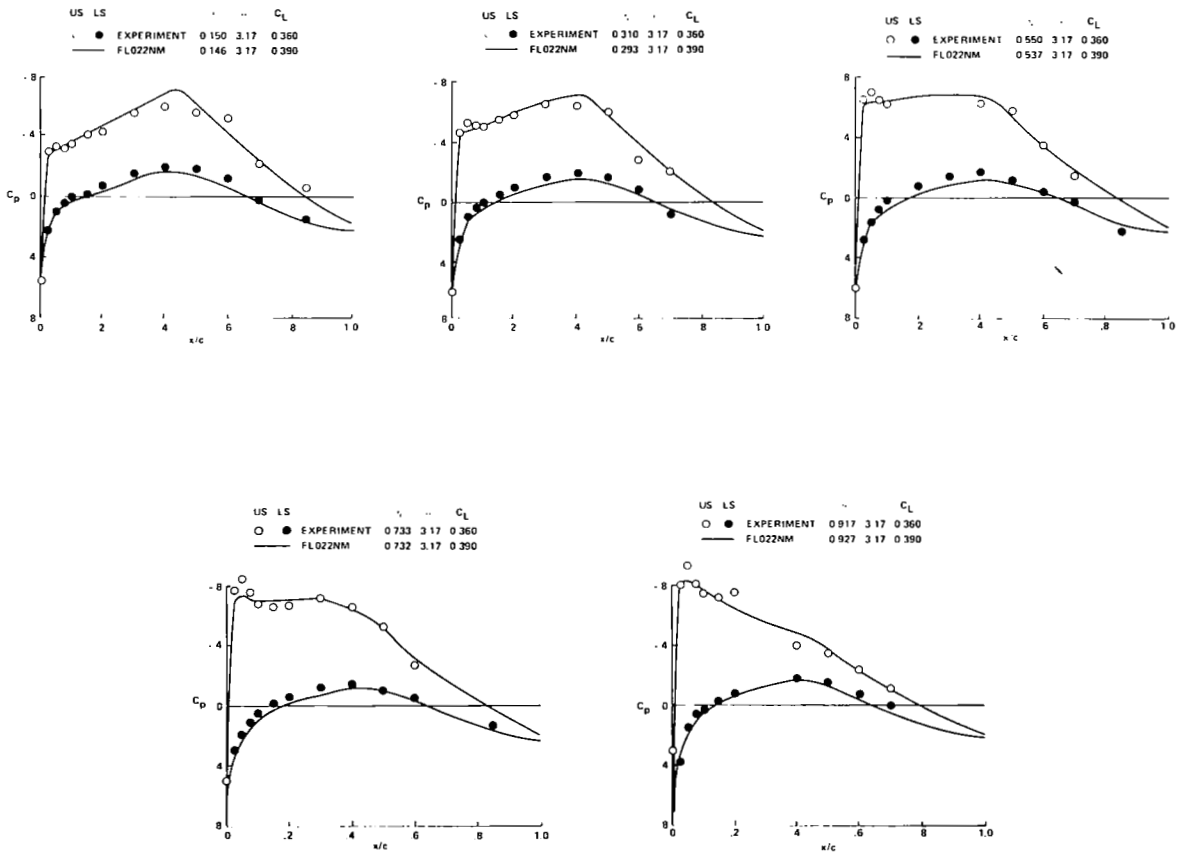

Figure 2

VOUGHT A-7 FIGHTER WIND TUNNEL MODEL

A model of the Vought A-7 fighter was tested in the Ames 11-foot transonic wind tunnel to evaluate the capability of FL022 to predict the surface pressures for a low aspect ratio wing mounted in the high position on a low fineness ratio body. A sketch of the wind tunnel model is shown in Figure 3. The wing has an average thickness of 12 percent of the chord.

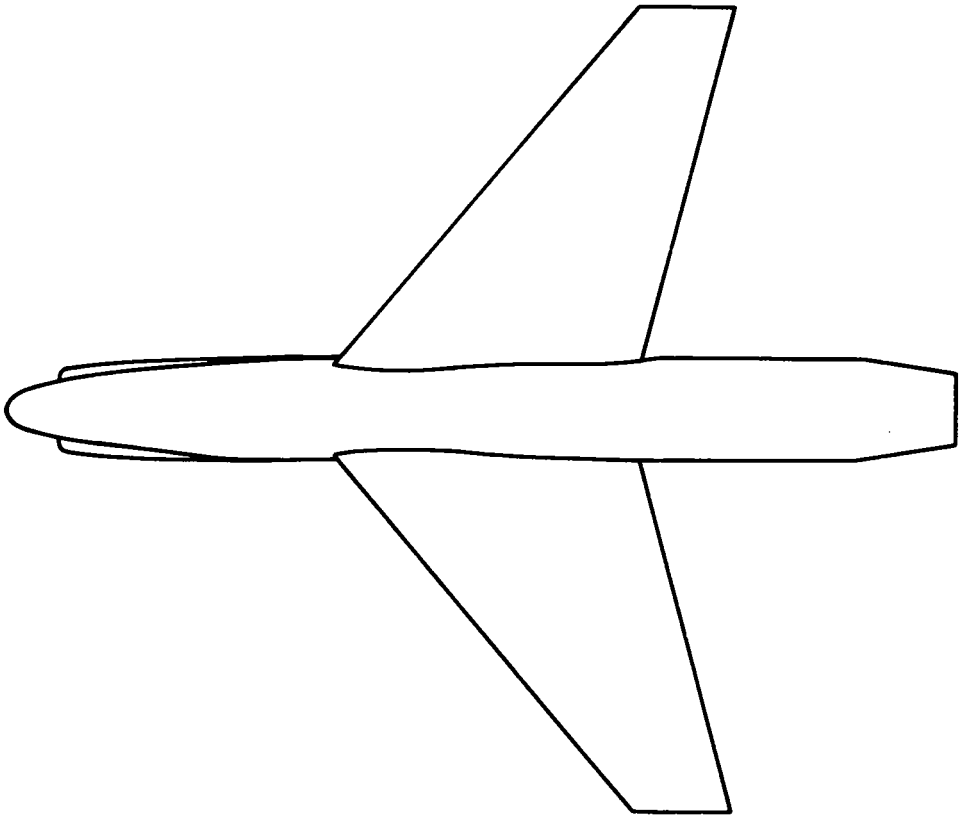

Figure 3

EXPERIMENT-THEORY CORRELATION FOR THE A-7 FIGHTER

The experiment-theory correlation for the A-7 fighter at Mach .85 and a Reynolds number of 8.7 million is shown in Figure 4. Note that FL022 predicts a shock position which is farther forward than the experiment at all span stations. The FL022 calculation includes a passive boundary layer correction but no body correction.

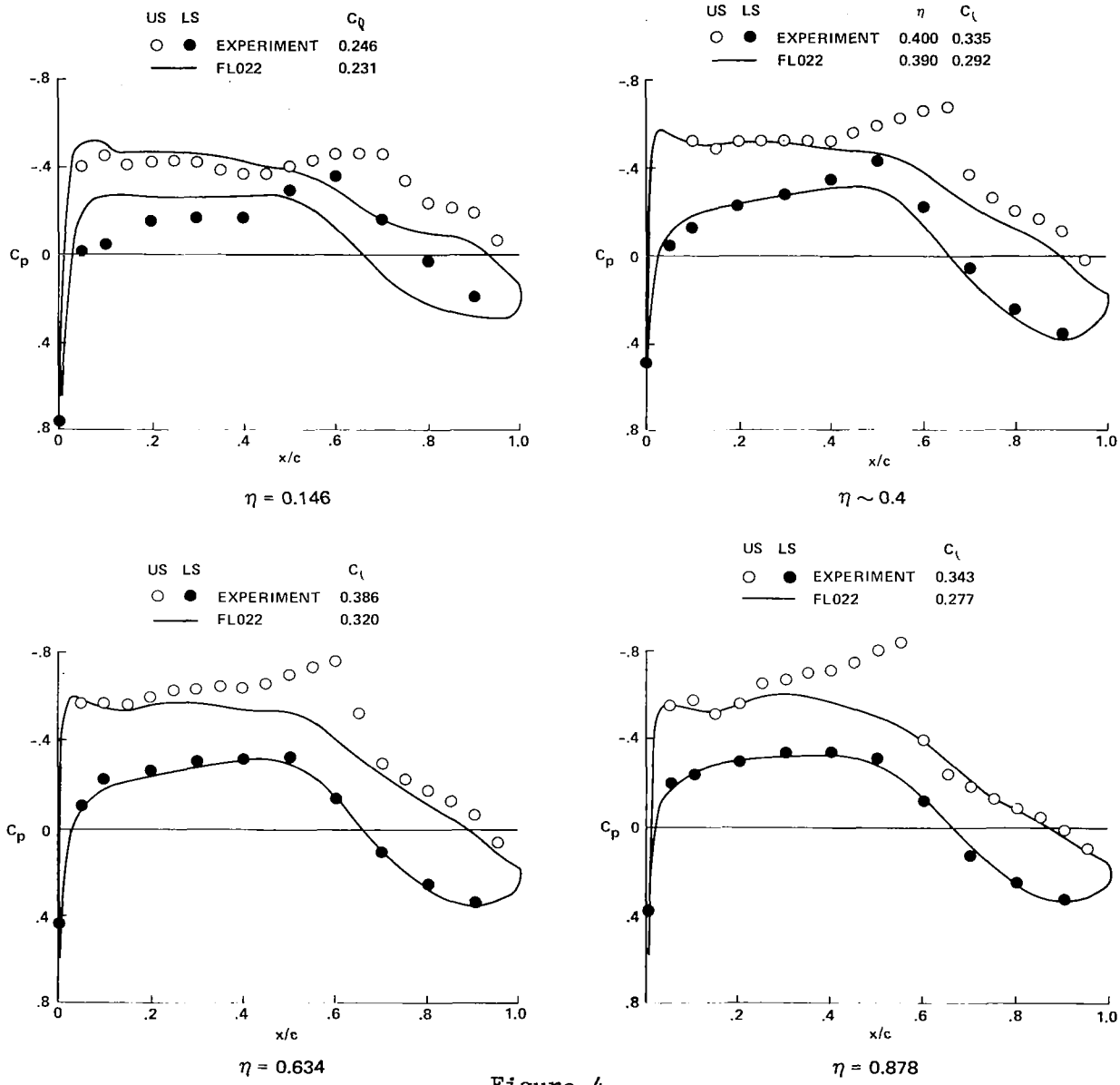

Figure 4

EXPERIMENT-THEORY CORRELATION FOR THE A-7 FIGHTER

A comparison of the A-7 wind tunnel data with calculations obtained from the wing-body code, FL028, is shown in Figure 5. Note that the shock position and strength predicted by FL028 agree well with the experimental values. The most serious flaw in the FL028 calculations is the pressure oscillations on the upper surface at the two inboard stations. This result indicates the importance of including the body effect in calculations involving this type of configuration.

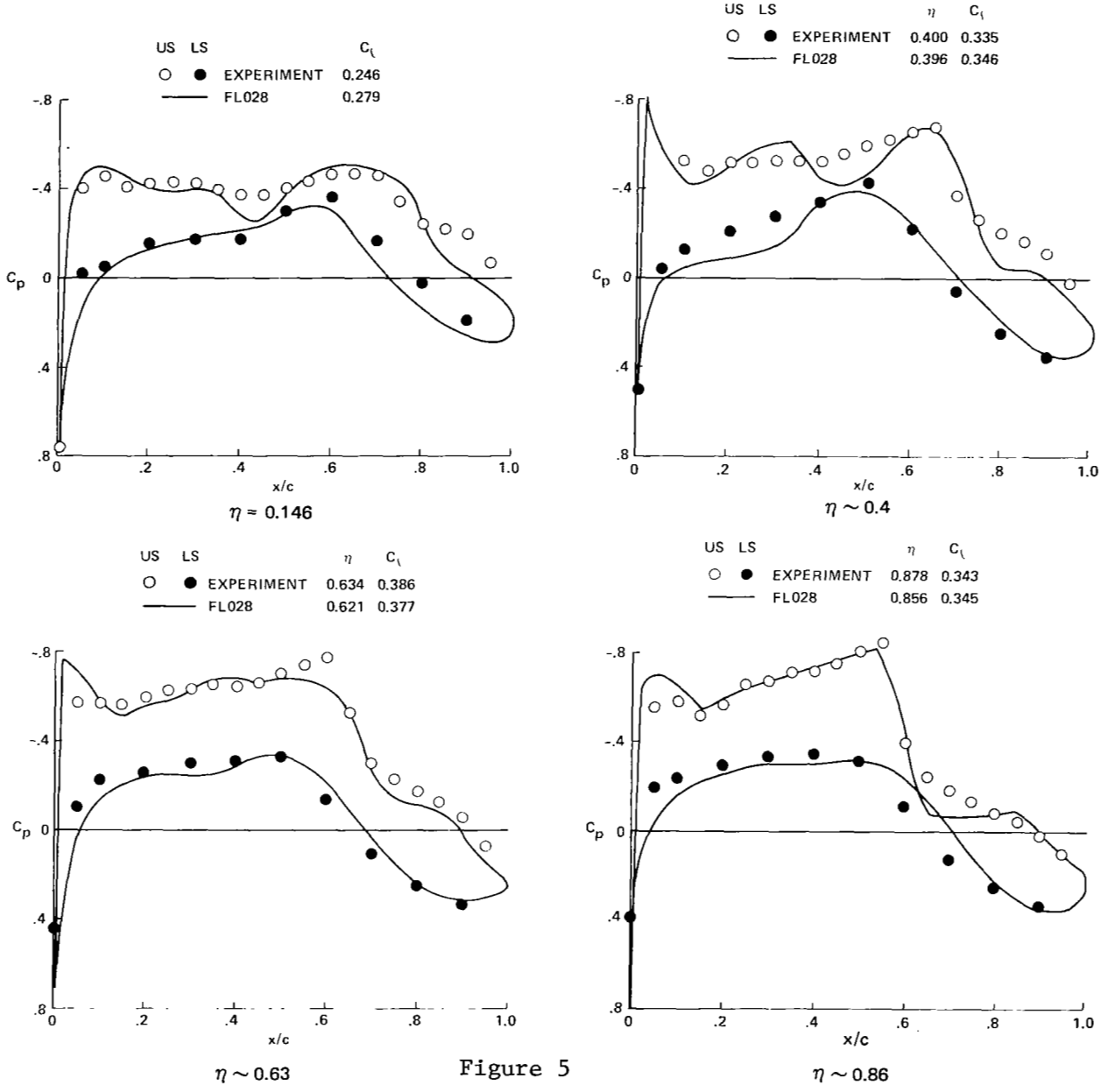

Figure 5

TRANSONIC WING-BODY WIND TUNNEL MODEL

The wind tunnel model shown in Figure 6 was tested in the Ames 14-foot transonic wind tunnel. This configuration has been included to show that the results shown previously for the A-7 fighter are not peculiar to high wing, low aspect ratio fighter aircraft.

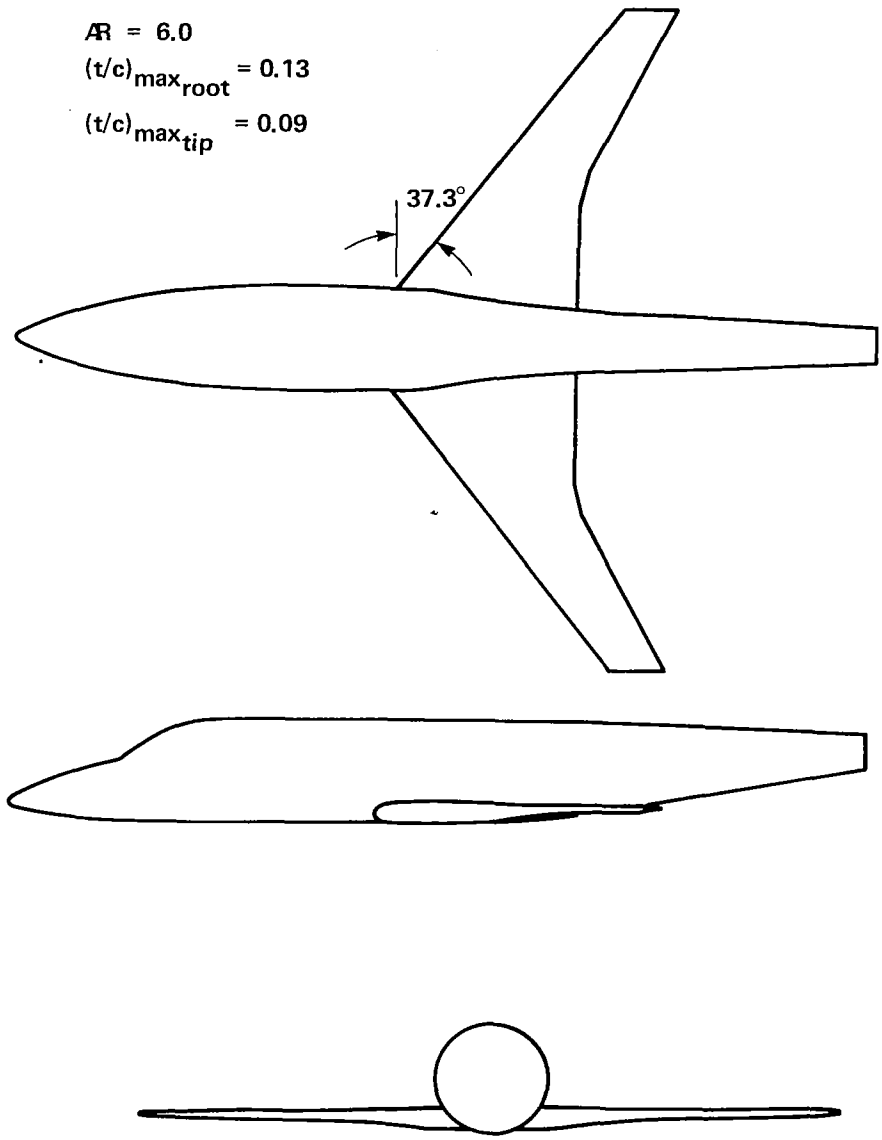

Figure 6

EXPERIMENT-THEORY CORRELATION FOR A TRANSONIC WING-BODY

A comparison of experimental wing pressures with those predicted by FL022 for Mach .8 and a Reynolds number of 2.3 million is shown in Figure 7 for a transonic wing-body configuration. The calculations included an iterated boundary layer correction and a twist distribution determined by a panel code analysis to correct for body effects. The poor correlation at the inboard stations indicates an inadquate body correction.

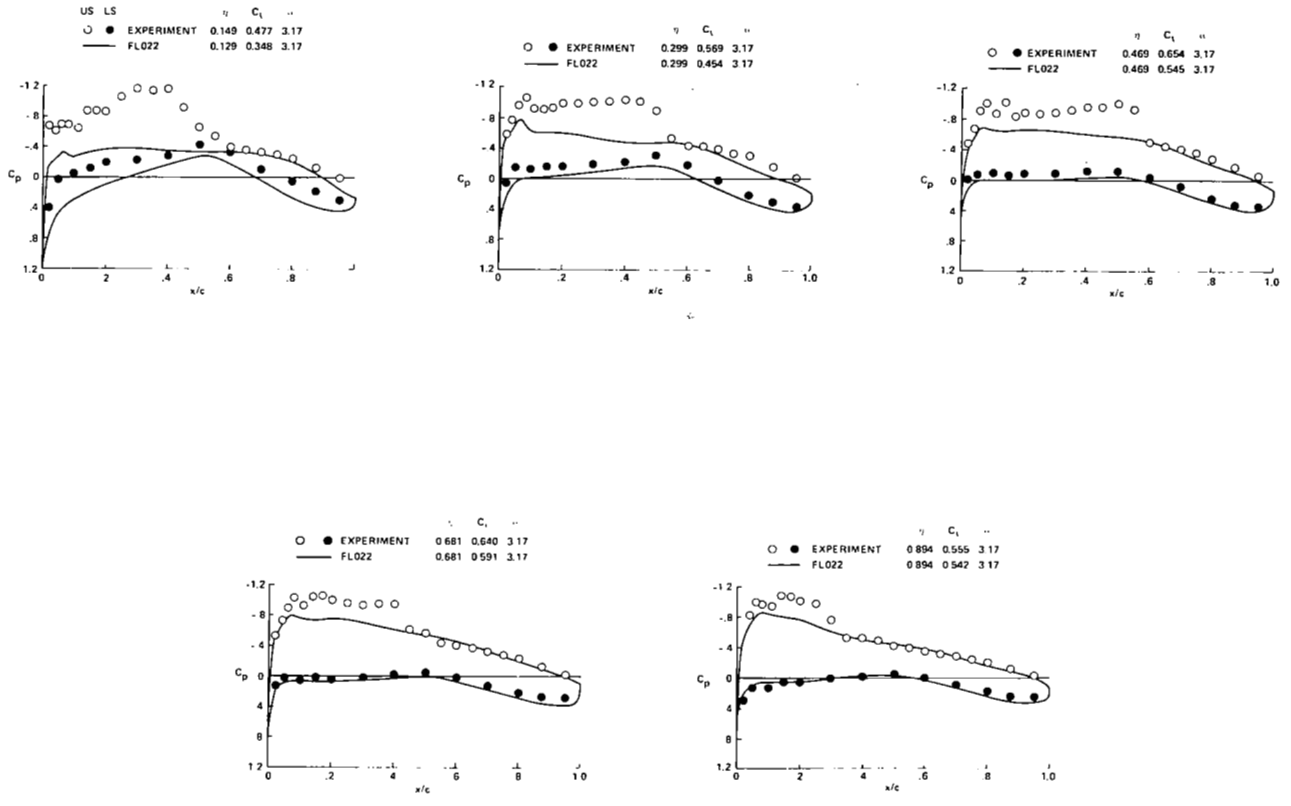

Figure 7

EXPERIMENT-THEORY CORRELATION FOR A TRANSONIC WING-BODY

The experimental pressures for the transonic wing-body configuration are compared with calculations from the wing-body code, FL030, in Figure 8. Note that the correlation is substantially improved over that observed with FL022 in Figure 7, particularly for the inboard stations.

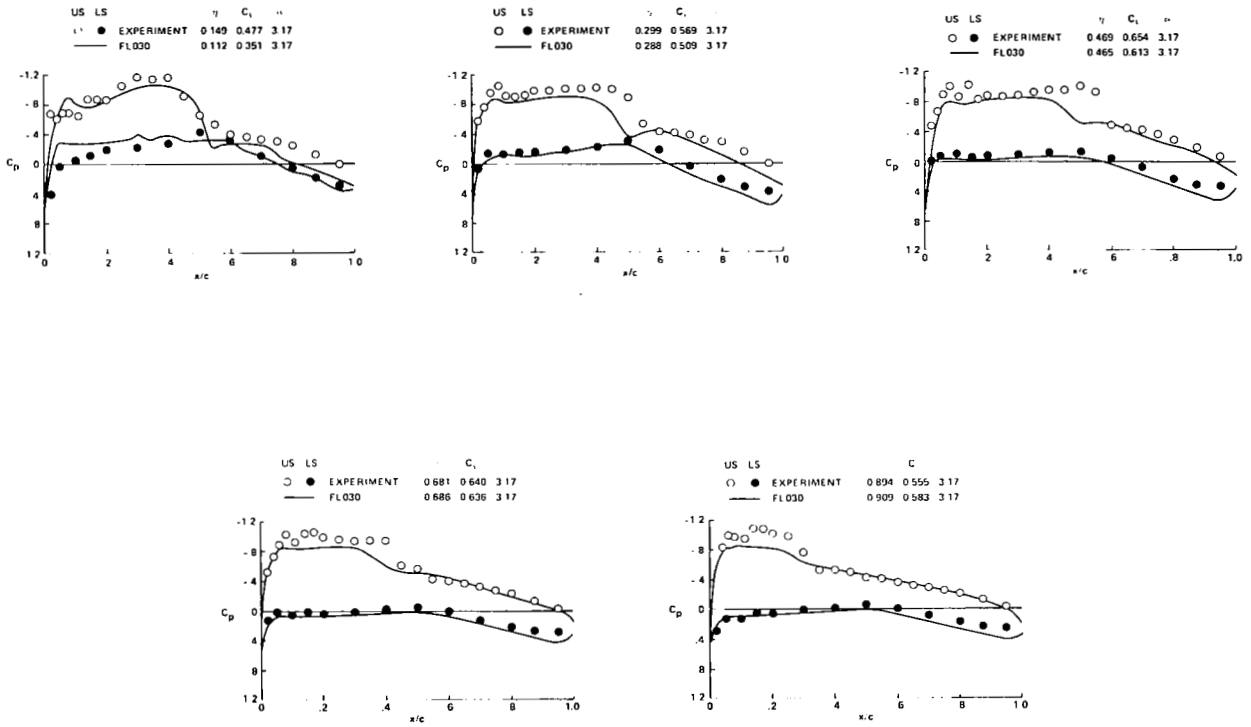

Figure 8

TRANSONIC BIZ-JET WIND TUNNEL MODEL

Tests of the transonic biz-jet configuration shown in Figure 9 permitted an evaluation of the ability of the wing-body code, FL028, to predict the effect of body mounted engines on the wing pressure distribution.

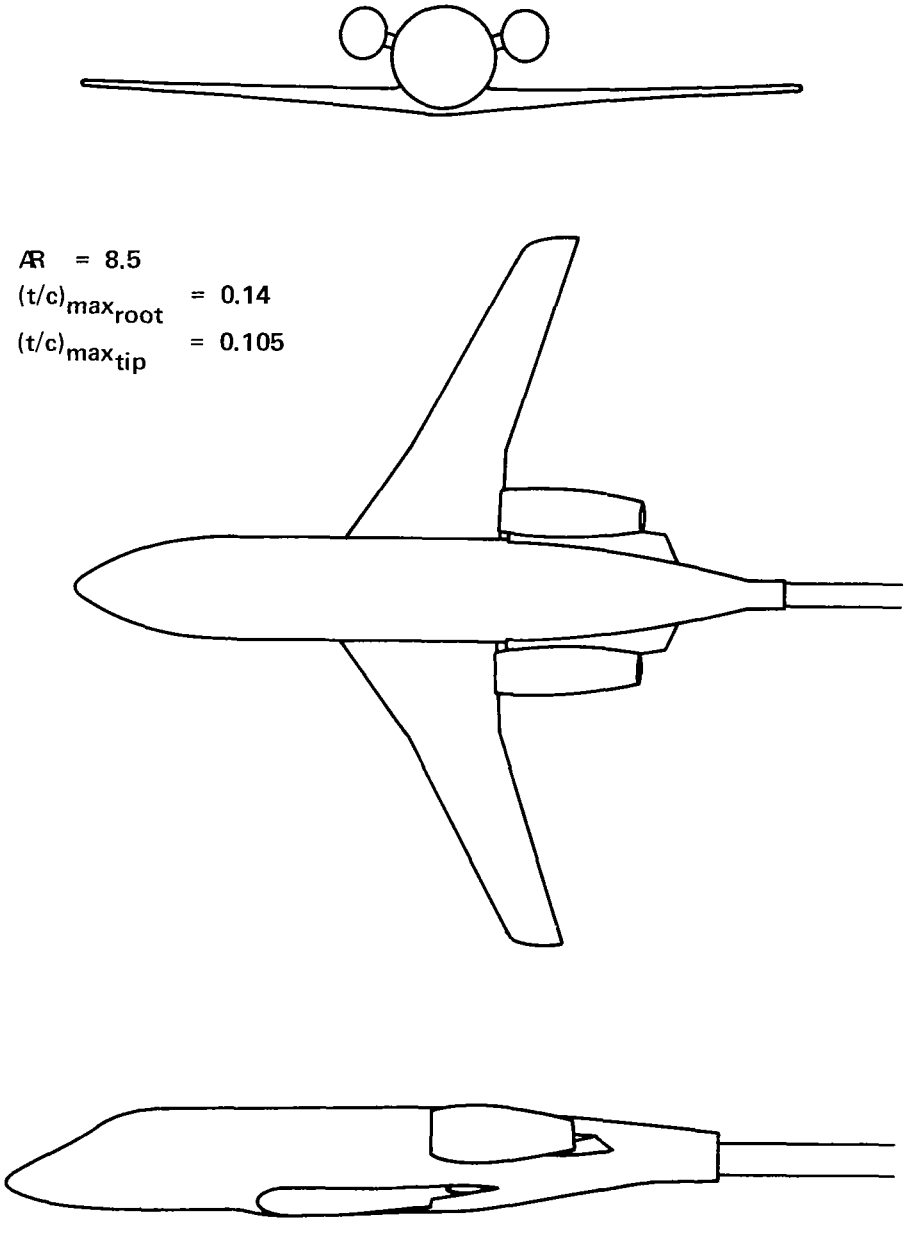

Figure 9

TRANSONIC BIZ-JET MATHEMATICAL MODEL

The mathematical model used to describe the transonic biz-jet configuration for input to FL028 is shown in Figure 10. The engine installation was simulated by a large "bump" on the side of the body with a cross-sectional area equal to the engine plus pylon minus capture area.

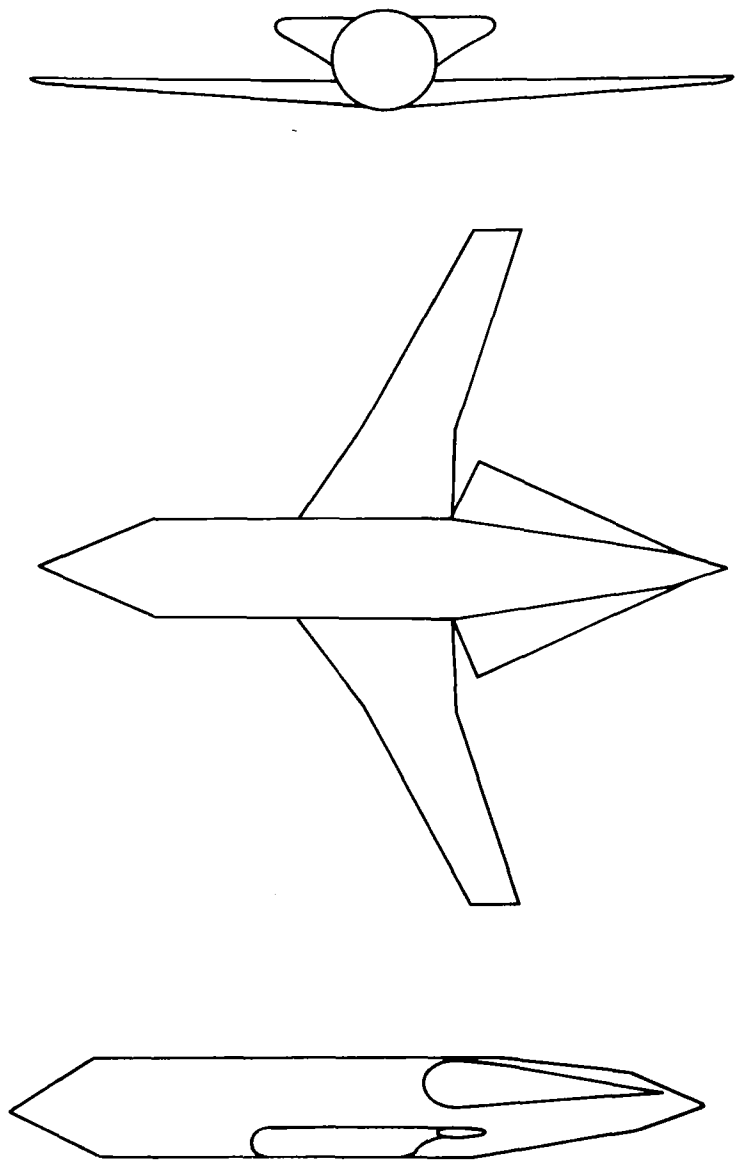

Figure 10

EXPERIMENT-THEORY CORRELATION FOR A TRANSONIC BIZ-JET

The experimental and theoretical pressure distributions with and without the engine installation are shown in Figure 11. The predicted pressures show the correct trend with engine installation but the magnitude of the effect is underestimated.

EXPERIMENT

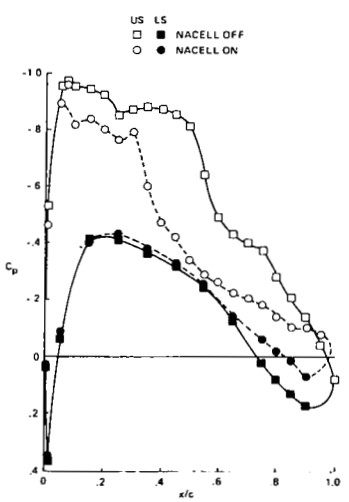

η = 0.27

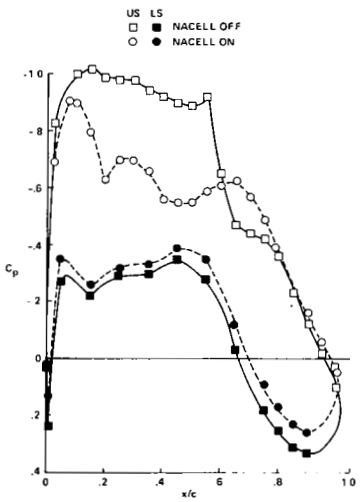

η = 0.55

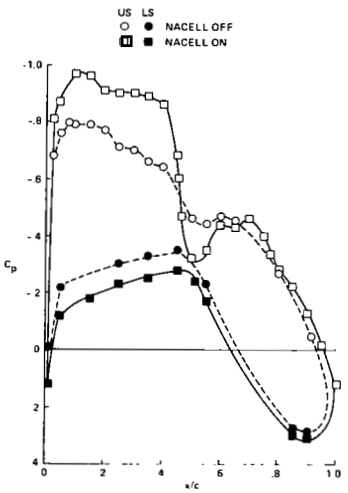

η = 0.85

THEORY

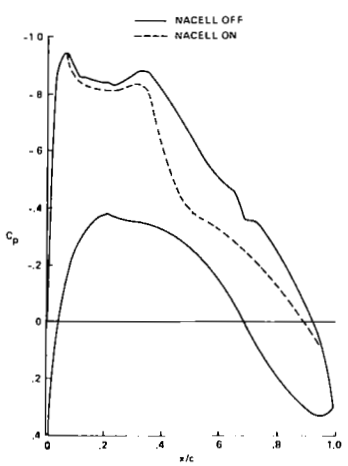

η = 0.27

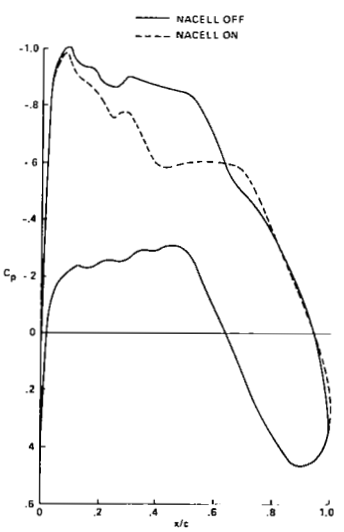

η = 0.55

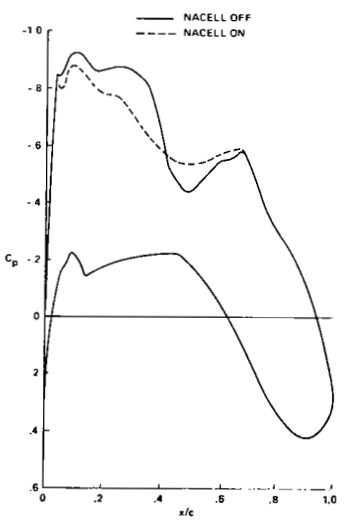

η = 0.85

Figure 11

REFERENCE

1. Edwards, George G.; and Boltz, Fredrick W.: An Analysis of the Forces and Pressure Distribution on a Wing with the Leading Edge Swept Back 37.25°. NACA RM A9K01, Mar. 1950.